

The **IT** University
of Copenhagen

Pre-Symmetry Set Based Shape Matching

Arjan Kuijper

Copyright © 2005, Arjan Kuijper

**IT University of Copenhagen
All rights reserved.**

**Reproduction of all or part of this work
is permitted for educational or research use
on condition that this copyright notice is
included in any copy.**

ISSN 1600-6100

ISBN 87-7949-106-5

Copies may be obtained by contacting:

**IT University of Copenhagen
Rued Langgaards Vej 7
DK-2300 Copenhagen S
Denmark**

Telephone: +45 72 18 50 00

Telefax: +45 72 18 50 01

Web www.itu.dk

Abstract

A novel shape descriptor is introduced. It groups pairs of points that share a geometrical property that is based on their mutual symmetry. The descriptor is visualized as a diagonally symmetric diagram with binary valued regions. This diagram is a fingerprint of global symmetry between pairs of points along the shape.

The descriptive power of the method is tested on a well-known shape data base containing several classes of shapes and partially occluded shapes. First tests with simple, elementary matching algorithms show good results.

1 Introduction

One method to describe 2D objects is by their outlines, or shapes. The complicated task of comparing objects then changes to comparing shapes. With a suitable representation, this task can be simplified. Several representations of shapes have been investigated in order to be able to perform this comparison efficiently and effectively. One of the earliest representations is Blum's skeleton [3], with the biological motivation that (say) the human skeleton is a reasonable representation of an human shape. As Kimia points out [6], there is evidence that humans use this type of representation.

Research on skeleton-based methods has been carried out in enormous extent ever since, see e.g. [9, 11]. The Shock Graph approach [15] has lead to a shape descriptor that can perform the comparison task very well [11, 13, 10]. This method depends on results obtained from so-called Symmetry Set [4, 5], a super set of the Medial Axis. In these cases, the shape is probed with circles tangent to it at at least two places. The Symmetry Set is obtained as the centres of all these circles, while the Medial Axis is the sub set containing only maximal circles.

From the field of robotics, probing shapes is also of interest. Blake et al. [2, 1] describe a grasping method by the set of points that are pair wise parallel. At such a pair a parallel jaw gripper can grasp the object. These points form the union of the symmetry set and a set they called anti-symmetry set, as it is closely related to the symmetry set.

In this work, we combine the ideas of these two fields of shape analysis by investigating the set of pairs of points at with a circle is tangent to the shape. We do not consider the centre of the circle, but the combination of the two points. A geometric method is given derive the pairs of points, based on a zero crossing argument. Therefore, to each pair of points a signed value can be assigned, yielding a matrix of values $(-1, 0, 1)$.

This matrix is then used as a shape descriptor. Its properties and allowed changes follow directly from the Symmetry Set, just as in the Shock Graph method. Next, a simple comparison algorithm is introduced to perform the task of object comparison. For this purpose, the two matrices for each pair of objects are set to equal dimensions and the normalized innerproduct is taken as equivalence measure. This procedure is tested on two data bases containing objects in different classes, where some objects are occluded or noisy. Given the simplicity of the algorithm, results are promising and erroneous results are due to the algorithm, showing the potential power of the representation.

2 Problem framework and definitions

The Medial Axis can be defined as the closure of the loci of the maximal circles tangent to a shape (see e.g. [5]). This somewhat abstract formulation can be made clear by investigation of Figure 1a. A circle with radius r is tangent to a shape at two points.

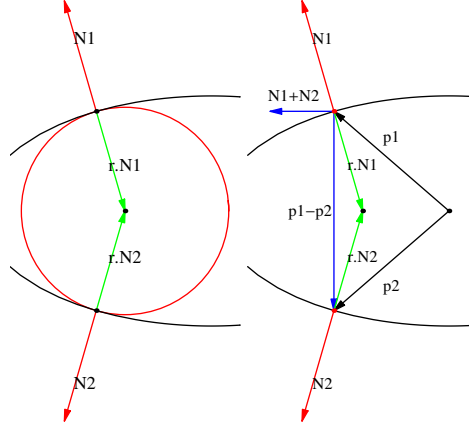


Figure 1: a) A pair of tangency points that gives rise to a Medial Axis point. b) The constellation of position and normal vectors is special at such points.

The unit length normal vectors (N_1 and N_2) of the circle and the shape coincide. The centre of the circle is a Medial Axis point, that is found by multiplying each normal vector with $-r$ and taking the tangency point as tail of the vector $-rN_i$. As there are for each point several combinations satisfying this tangency argument¹, the set is taken for with $-r$ is maximal, i.e. the set with the smallest radius.

The two points can be found using geometrical arguments [4], see Fig. 1b. Take an arbitrary origin point and let p_1 and p_2 be vectors pointing to the two locations of tangency. Then $p_1 - p_2$ is a vector pointing from one tangency point to the other. From the construction of the circle as described before, the vector $-rN_1 + rN_2$ (and when normal vectors are pointing inward and outward $-rN_1 - rN_2$) is parallel to $p_1 - p_2$. Consequently $(p_1 - p_2) \cdot (N_1 \pm N_2) = 0$ for these two points. Let a shape be continuously parameterized then for each point p several points q_j can be found for which

$$(p - q_j) \cdot (N(p) \pm N(q_j)) = 0 \quad (1)$$

where $N(\cdot)$ denotes the normal vector. Note that if the normal vectors are parallel, the inner product is zero as well. Such points are the anti-Symmetry Set points described by Blake et al. [2, 1] for the parallel jaw gripper. If the shape is parameterized by N points (p_1, p_2, \dots, p_N) , then the tangency pairs are found as the zero crossings of Eq. 1. To find these zero crossings, it suffices to look at the square sign-of-innerproduct diagram $P(i, j)$ of the signed values of Eq.1:

$$P(i, j) = \text{sign} [(p_i - p_j) \cdot (N_i \pm N_j)] \quad (2)$$

In Figure 2 a fish shape is shown, together with its sign-of-innerproduct diagram. When actual zero crossings are computed, i.e. when the boundaries of the regions in such a diagram are taken, one obtains a so-called pre-Symmetry Set that is used to derive the distinct branches of the Symmetry Set [4, 8]. The possible changes of these boundaries when the shape changes, are known [7] and relate to the possible changes of the Medial Axis [5].

Changes in the shape lead to movement of the boundaries and therefore to changes of areas. Topological changes fall apart into two classes: Firstly, boundaries can meet

¹It can be shown that for each point there are at least two other points [4]. Constellations with tangency normal vectors pointing inside and outside can occur [5].

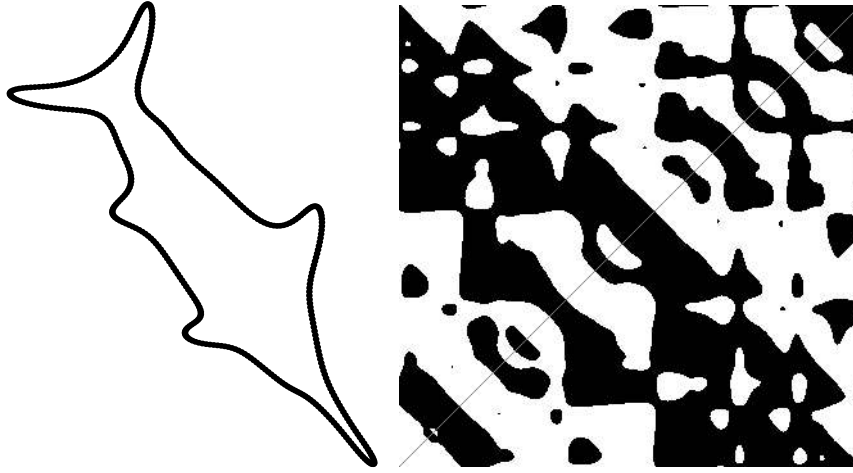


Figure 2: a) A fish shape. b) Sign-of-innerproduct diagram for the fish shape.

and establish a different connection when a white (or black) region is locally split into two parts. Secondly, regions can be annihilated or created, either on the diagonal or pair-wise off-diagonal. Other possible changes of the Symmetry Set do not lead to topological changes.

As may be clear from Eq. 2b, the diagram is symmetric in the diagonal. It can be identified with the shape, just as (by definition) the axes of the diagram. The values on the diagonal equal zero, as these points cannot be evaluated in Eq. 1. Second, on all other point combinations it is non-generic to encounter exactly a zero-crossing, so either a positive or a negative sign is obtained.

3 Sign-of-innerproduct diagram based matching

The task of comparing objects has now become the task of comparing diagrams. If the parameterizations of two shapes consist of the same amount of points n , the corresponding sign-of-innerproduct diagrams can be multiplied element wise with each other. If the shapes are identical and the parameterizations are equal, this innerproduct equals $n(n - 1)$, since the diagonal consists of n points.

If the parameterizations are taken at a different starting position, so that $p_i = q_{i+\alpha}$, rotated version of the sign-of-innerproduct diagram should be taken into account. This rotation takes place in horizontal and vertical directions simultaneously, as $P(i, j) = Q(i + \alpha, j + \alpha)$, values taken modulo n . So to validate each possible starting position, n instances need to be compared.

Finally, the number of points for both shapes need not be equal. If the difference is m rows (and columns), a method must be chosen that removes m rows and columns. One choice is to remove them equally spread over the largest sign-of-innerproduct diagram. This relates to removing a set of equidistant points along shape with the largest number of points. It can be regarded as a re-parameterization of the shape with the largest number of points.

Now let two shapes S_1, S_2 be parameterized with n_1 and n_2 points. Assume without loss of generality $n_1 \leq n_2$. The sign-of-innerproduct diagram of S_2 is denoted by P_1 . Let $n = n_1$ and $m = n_2 - n_1$. Build P_2 by removing each $(\frac{m}{n_2})^{th}$ row and column of the sign-of-innerproduct diagram of S_2 . Let P_1^r denote the sign-of-innerproduct diagram P_1 considered with as starting position point r on the shape, i.e. P_1 with its

first $r - 1$ columns and rows transferred to positions $n + 1, \dots, n + r - 1$:

$$P_1^r(i, j) = P_1(i - r + 1, j - r + 1),$$

where values are taken modulo n . This matches the shapes regardless of begin position of the parameterizations. Then the matching $D(P_1, P_2)$ between S_1, S_2 is set as

$$D(S_1, S_2) = \max_r(D(S_1^r, S_2)) \quad (3)$$

with

$$D(S_1^r, S_2) = \frac{\sum_{i=1}^n \sum_{j=1}^n P_1^r(i, j) P_2(i, j)}{n(n-1)} - \frac{m}{2n_2} \quad (4)$$

The first term in Eq. 4 denotes the weighted equality of the two sign-of-innerproduct diagram P_1^r, P_2 . Perfect match is given by 1, while a complete mismatch equals -1 and a random match 0. The second term penalizes the difference in number of points in a parameterization, as this difference is ignored in the first term by construction.

4 Data Base Matching

As first test set three classes from an online data base are taken². The classes contain fishes, planes, and tools. Some fishes and planes are artificially drawn, and some form interclass instances. The results of the matching algorithm can be seen in Figures 3a,b. The first column contains the shape that is compared to all other shapes. The score is zero, as it matches to itself without difference. The second column gives the second best match, etc.

The matching is consistent with [14], where this database is introduced. One can see, for instance, that tools match to tools, and that the wrenches and double wrenches match to the correct set. The erroneous matches – the appearances of shapes of a different class – occur at a match $D = .5$ or less. These errors can visually be explained: A coarse plane “looks” like a fish with two big fins.

Next, this approach is used on the data base used by Sebastian et al. [12]. This data base contains 9 classes with 11 shapes each. Some of the shapes are occluded or deformed versions of another shape in the class. Just as in [12], a score $D^*(S_1, S_2)$ is set to be a non-negative number, ranging towards 1000. This is achieved by taking (recall Eq. 3)

$$D^*(S_1, S_2) = 1000(1 - D(S_1, S_2)) \quad (5)$$

Now 0 denotes a perfect match and values towards 1000 a random match. The results per class are shown in Figs. 4-8.

In each of the figures, the first column resembles the shape matched with itself, resulting in a score of 0. The next 10 columns give the second to eleventh best match. Ideally, this would be shapes from the same class. The score of each shape is taken as an eleven dimensional vector with each value being zero or one. A one at position i denotes a shape at the i^{th} position that belongs to the same class, while a zero denotes a shape of a different class. The total class score is then given as the sum of the eleven vectors in the class, ideally being a vector containing 11 elevens. Table 1 gives these results.

5 Discussion of results

Table 1 shows that some classes (6 and 9) yield a perfect score. Other classes contain matchings to objects of other classes. For some this occurs at higher positions, but in three cases already the second best match is wrong.

²<http://www.lems.brown.edu/vision/researchAreas/SIID/>

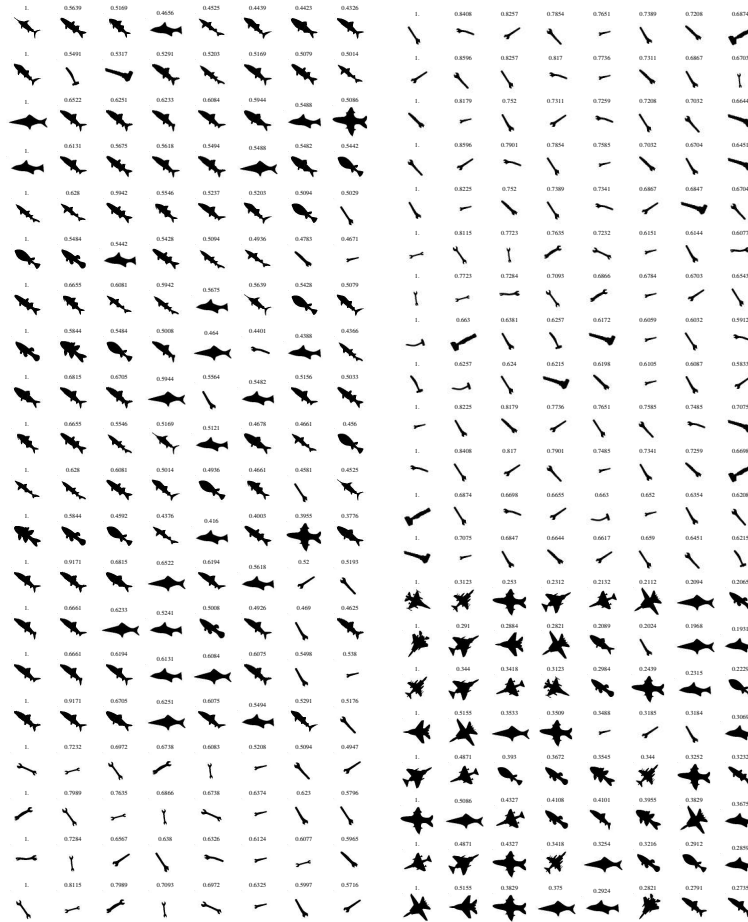


Figure 3: Matching of fishes, tools, and planes.

All these cases are caused by the choice of the matching algorithm, the removal of equidistant points. This is strongest visible in the third class, top of Fig. 5. The 9th row introduces a shape that has a large occlusion. This relates to removing a set of neighbouring points along the shape instead of the taken approach. An indication that “something is wrong” is given by the high cost for the second best match (620), compared to the other second best matches in this class (≤ 269). Is introduces a complete row of wrong matches.

A similar effect, albeit in the opposite way, occurs in the fifth class, top of Fig. 6. The third row shows an occluded hand, which relates to a local addition of a set of neighbouring points along the shape. Again a high cost for the second best match is obtained. Assuming only equidistant removal of points, however, the second best match is visually correct. The fingers correspond to the four legs of the cow, while the blown-up thumb relates to the cow’s head and body. The same thing can be said about the occluded rabbit in class 8, Fig. 7 bottom.

Obviously, the human classification is not perfectly mimicked by the algorithm. The total amount of errors compared to the human observer classification is given by (0, 3, 6, 6, 12, 17, 24, 28, 42, 43, 58). If the three most clear occlusion-caused outliers are left out, this is (0, 0, 3, 5, 9, 15, 22, 25, 39, 41, 56).

As a way to avoid the removal of points in one of the sign-of-innerproduct diagram, one can obtain a parameterization of exactly n points. This results in more

class	score
1	11,11,11,11,11,11,11,8,6,7,1
2	11,11,9,10,8,6,8,5,4,5,2
3	11,10,10,10,10,10,9,8,9,7,2
4	11,11,11,10,10,8,9,10,7,6,3
5	11,10,9,9,7,8,1,2,0,3,6
6	11,11,11,11,11,11,11,11,11,11,11
7	11,11,11,10,10,8,6,8,2,3,3
8	11,10,10,11,9,9,9,8,7,3,2
9	11,11,11,11,11,11,11,11,11,11,11

Table 1: Score of inter-class matches.

or less the same outcome, since it still does not take into account the effects of occlusion. Secondly, forcing a standard number of points along the shape wipes out the complexity of shape, so the matching actually yields worse results.

First attempts have been made in order to remove a set of $\frac{m}{n_2}$ locally neighbouring points. For the occluded human figure, this yielded a better matching to other human shapes. It is, however, computationally very expensive implemented. To compare two shapes takes approximately tens of minutes, compared to several seconds in the equidistant case. However, as the optimal match is a summation of a set of multiplications, a fast dynamic program may be available. In this case the task would be to find a shortest manifold in 4D.

6 Summary and Conclusions

A new shape descriptor is introduced. It is based on pairs of points on the shape that lie on a circle that is tangent to the shape at these points. It is therefore closely related to both Medial Axis and Symmetry Set methods. Each point on the shape is compared to all other points on the shape regarding a geometrical relation. Based on this, to each pair of points a value $+1$ or -1 is assigned. This yields an efficient data structure.

Secondly, shapes can be compared using this data structure. As test, a general data base [12] was used, containing shapes in different classes. Some of the shapes are severely occluded. To compare two data structures, the used approach removed a set of equidistant points along the shape, thus enforcing two shapes parameterized with the same number of points. This allows simple comparison of two data structures.

Although this matching assumption is very general and a priori not suited for occluded shapes, results were relatively good. The comparison of two shapes can be done in few seconds, using non-optimized Mathematica code. Some shape classes were completely correct classified, while other had a correct score for most of the shapes. The shapes that significantly scored bad were shapes with a large blocked occlusion, or with a locally removed part. These parts cannot be matched correctly by definition with the used method. We note that these deformed shapes give a relatively simple different Medial Axis. Secondly, we only matched one shape to another, allowing the changes to appear in only one shape. In general, the matching involves changes to both shapes, for example in matching the hands of class 5 (see Fig. 6, top) with different occluded fingers.

An obvious amendment of the matching algorithm is the possibility of removing a set of neighbouring points. This will solve the problem of occluded parts, both where a part of the shape is removed, and where a part (a block) is added. Second, the method is to be designed to find the optimal solution allowing both data structure

to be changed. As the optimal match is a summation of a series of multiplications, a fast shortest-path based dynamic program may be available to incorporate these two amendments simultaneously. Current work includes this task finding a shortest manifold in 4D.

References

- [1] A. Blake and M. Taylor. Planning planar grasps of smooth contours. *Proceedings IEEE International Conference on Robotics and Automation*, pages 834–839 vol.2, 1993.
- [2] A. Blake, M. Taylor, and A. Cox. Grasping visual symmetry. *Proceedings Fourth International Conference on Computer Vision*, pages 724–733, 1993.
- [3] H. Blum. Biological shape and visual science (part i). *Journal of Theoretical Biology*, 38:205–287, 1973.
- [4] J. W. Bruce, P. J. Giblin, and C. Gibson. Symmetry sets. *Proceedings of the Royal Society of Edinburgh*, 101(A):163–186, 1985.
- [5] P. J. Giblin and B. B. Kimia. On the local form and transitions of symmetry sets, medial axes, and shocks. *International Journal of Computer Vision*, 54(1/2):143–156, 2003.
- [6] B.B. Kimia. On the role of medial geometry in human vision. *Journal of Physiology - Paris*, 97(2-3):155–190, 2003.
- [7] A. Kuijper and O.F. Olsen. Transitions of the pre-symmetry set. In *Proceedings of the 17th International Conference on on Pattern Recognition*, volume III, pages 190–193, 2004.
- [8] A. Kuijper, O.F. Olsen, P.J. Giblin, Ph. Bille, and M. Nielsen. From a 2D shape to a string structure using the symmetry set. In *Proceedings of the 8th European Conference on Computer Vision*, volume II, pages 313–326, 2004. LNCS 3022.
- [9] R. L. Ogniewicz and O. Kübler. Hierarchic voronoi skeletons. *Pattern Recognition*, 28(3):343–359, 1995.
- [10] M. Pelillo, K. Siddiqi, and S. Zucker. Matching hierarchical structures using association graphs. *IEEE Transactions on Pattern Analysis and Machine Intelligence*, 21(11):1105–1120, 1999.
- [11] T.B. Sebastian and B. B. Kimia. Curves vs. skeletons in object recognition. *Signal Processing*, 85(2):247–263, 2005.
- [12] T.B. Sebastian, P.N. Klein, and B. B. Kimia. Recognition of shapes by editing shock graphs. In *Proceedings of the 8th International Conference on Computer Vision*, pages 755–762, 2001.
- [13] T.B. Sebastian, P.N. Klein, and B. B. Kimia. Recognition of shapes by editing shock graphs. *IEEE Transactions on Pattern Analysis and Machine Intelligence*, 26(5):550–571, 2004.
- [14] D. Sharvit, J. Chan, H. Tek, and B.B. Kimia. Symmetry-based indexing of image databases. *Journal of Visual Communication and Image Representation*, 9(4):366–380, 1998.
- [15] K. Siddiqi and B.B. Kimia. A shock grammar for recognition. *Proceedings CVPR '96*, pages 507–513, 1996.



Figure 4: Classes 1 and 2.

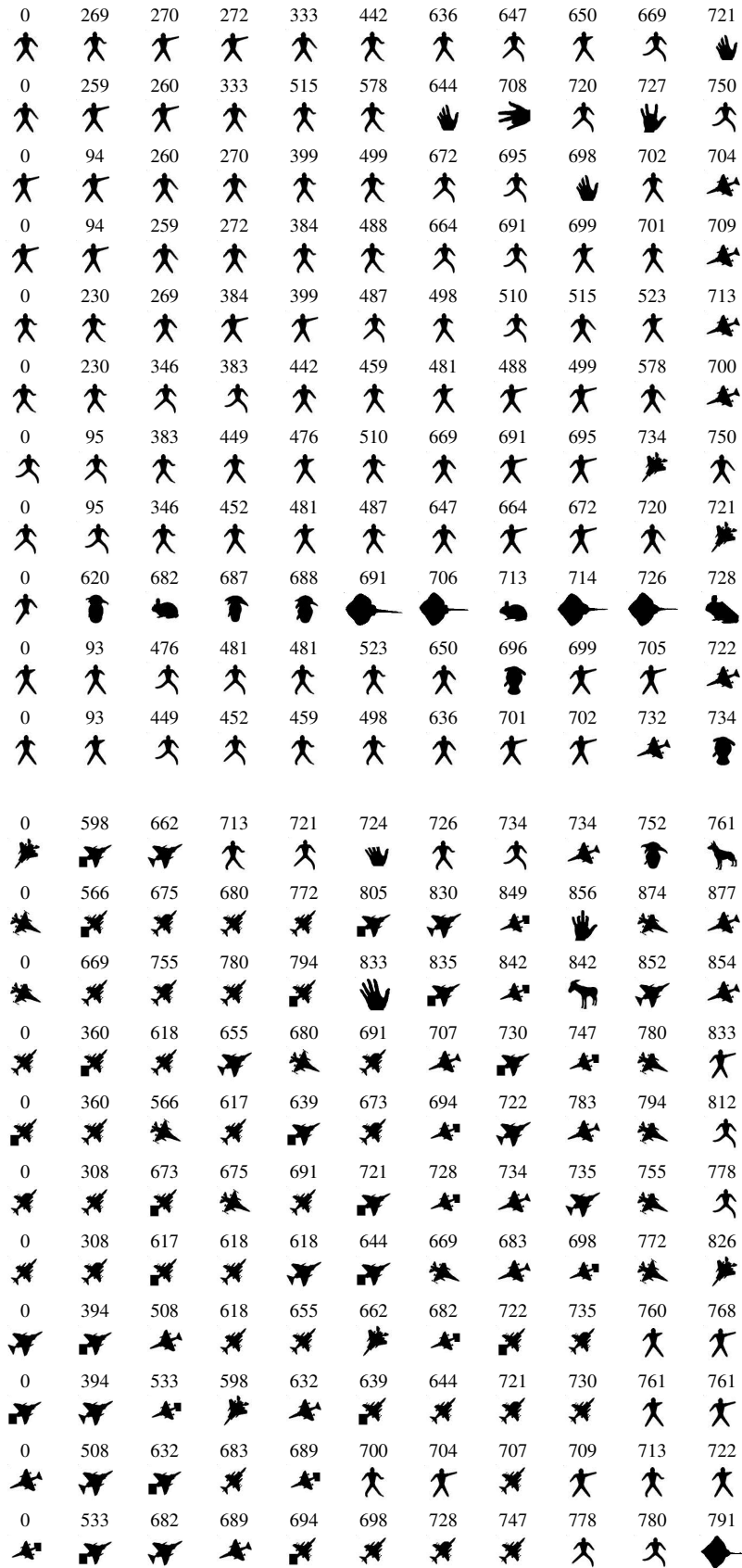


Figure 5: Classes 3 and 4.

0	3	253	309	488	560	780	785	848	848	855
0	304	309	358	443	646	763	795	798	818	825
0	842	900	902	916	917	918	954	965	969	969
0	630	715	724	756	758	761	772	780	787	805
0	614	644	681	698	710	721	743	769	772	786
0	358	560	562	591	694	737	781	782	840	849
0	3	254	304	488	562	779	786	847	848	855
0	253	254	443	496	591	809	842	862	883	897
0	488	488	496	646	694	795	807	827	839	848
0	334	630	681	727	783	789	789	802	803	809
0	334	614	708	715	781	787	787	788	791	818
0	196	215	215	219	234	241	262	327	361	527
0	227	283	301	327	372	376	381	397	471	583
0	247	260	267	274	342	347	348	361	411	471
0	198	214	221	236	260	262	291	299	376	418
0	221	234	262	289	291	301	301	307	342	473
0	180	194	214	215	236	266	274	307	372	452
0	219	221	236	236	262	274	283	296	348	502
0	215	221	227	236	266	283	283	299	411	518
0	347	373	405	418	452	473	502	518	527	583
0	130	180	196	198	247	274	283	289	381	405
0	130	194	236	241	267	283	296	301	373	397

Figure 6: Classes 5 and 6.



Figure 7: Classes 7 and 8.

0	189	193	219	330	417	456	515	533	573	578
0	189	225	262	320	373	406	438	489	493	502
0	219	225	228	337	339	395	438	457	459	471
0	255	393	406	413	427	438	453	455	456	484
0	193	228	262	278	393	445	519	549	577	592
0	160	230	243	266	455	471	502	505	577	578
0	160	230	259	293	453	459	493	497	573	592
0	216	228	259	266	337	373	413	417	445	478
0	255	278	320	330	339	478	497	505	520	535
0	216	243	287	293	395	438	484	515	519	520
0	228	230	230	287	427	457	489	533	535	549

Figure 8: Class9.